Journal of the Korean Nuclear Society
Volume 33, Number 3, pp.298~306, June, 2001

Static Structural Analysis on the Mechanical behavior of the KALIMER Fuel Assembly Duct

Kyung Gun Kim, Byoung Oon Lee, Woan Hwang, and Young Il Kim
Korea Atomic Energy Research Institute
150 Dukjin-dong, Yusong-gu, Taejon 305-353, Korea
Yong su Kim
Hanyang University
17 Haengdang-dong, Sungdong-gu, Seoul 133-791, Korea

(Received September 29, 2000)

Abstract

As fuel burnup proceeds, thermal gradients, differential swelling, and inter-assembly loading may induce assembly duct bowing. Since duct bowing affects the reactivity, such as long or short term power-reactivity-decrement variations, handling problem, caused by top end deflection of the bowed assembly duct, and the integrity of the assembly duct itself. Assembly duct bowing were first observed at EBR-II in 1965, and then several designs of assembly ducts and core restraint system were used to accommodate this problem. In this study, NUBOW-2D KMOD was used to analyze the bowing behavior of the assembly duct under the KALIMER(Korea Advanced LIquid MEtal Reactor) core restraint system conditions. The mechanical behavior of assembly ducts related to several design parameters are evaluated. ACLP(Above Core Load Pad) positions, the gap distance between the ducts, and the gap distance between the duct and restraint ring were selected as the sensitivity parameter for the evaluation of duct deflection.

Key Words : static structural analysis, bowing, duct, restraint system, HT9, NUBOW, FEM, limited-free bowing system

1. Introduction

Thermal gradients, differential creep and swelling, and inter-assembly loading may induce assembly duct bowing under an LMFBR(Liquid Metal Fast Breeder Reactor) environment. Assembly duct bowing refer the displacement of the top assembly duct inward or outward from a straight duct[1,2]. At the beginning of burnup, since high temperature exist near the core region thermal bowing of duct developed due to thermal expansion of duct material(HT9, ferritic martensitic stainless steel) and additional inelastic swelling of duct developed gradually. Although, when temperatures go down, thermal bowing is disappeared because thermal bowing is a elastic

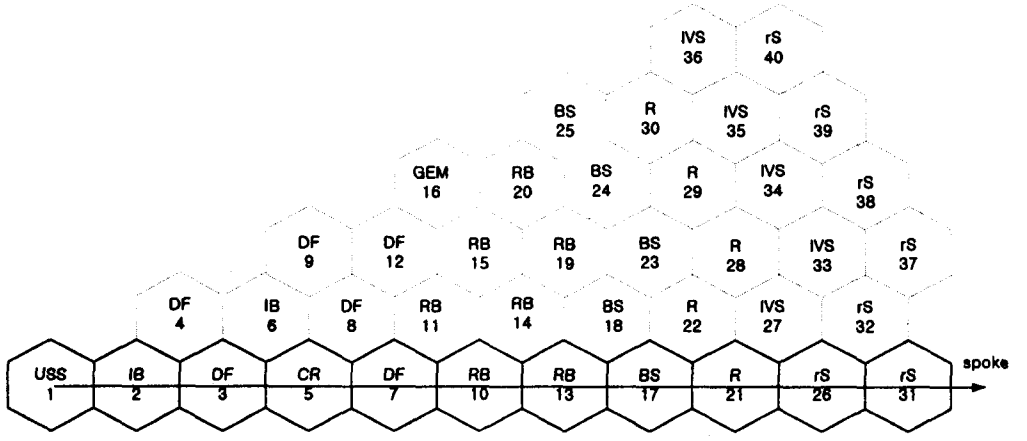

Fig. 1 KALIMER Core Arrangement

deformation component, but inelastic swelling bow is remained. When thermal and swelling bowing is larger than the interduct gap distance, interaction between the assembly ducts may occur. The interaction forces by thermal and swelling bow produce stresses in the assembly duct wall. Irradiation-induced creep relaxes these stresses and inelastic creep deformation developed. As a result, the interaction forces between ducts are reduced. KALIMER core arrangement showed Fig. 1 where each DF(Driver Fuel assembly duct), IB(Inner Blanket assembly duct), RB(Radial Blanket assembly duct), CR(Control Rod assembly duct), BS(B4C Shield assembly duct), R(Reflector assembly duct), and rS(radial Shield assembly duct) have fuel rod, blanket rod, control rod and shield rod. And USS is Ultimate Shout-down System. Since relatively high temperature and flux gradients exist near the interface of the fuel assembly duct and radial blanket duct regions, the largest inelastic bow due to the differential creep may occur in this region. Assembly ducts cluster may occur in this region, and the magnitude of bow and assembly duct stiffness in addition overall assembly cluster tightness may excess removal load. Assembly duct bowing at the core region may causes significant reactivity changes and difficulties in removing an individual duct from their grid position in the core. As previously described, it In each country, core element deflection analysis codes such as CRAMP[3], DDT[4], ARKAS[5] etc. have been developed for their LMFBR program. In this study, the NUBOW-2D Inelastic developed by ANL[6] upgraded to NUBOW-2D KMOD and used to analyze the bowing behavior of the assembly duct under KALIMER core restraint system conditions where KALIMER is based on Limited Free Bow core restraint system[7]. Limited Free Bow core restraint system refer the outward deflection of assembly duct were restrained by restraint ring(see Fig. 2). In addition, Free Flowering core restraint system installed strong stiffness duct to outer core to restrain outward deflection of assembly duct. In order to describe the behavior of the assembly duct and core restraint system properly, a three-dimensional code[8] is required for the core design and operational management. Hence, this study is as a basic study for a three dimensional analysis in the future for the core structural analysis code.

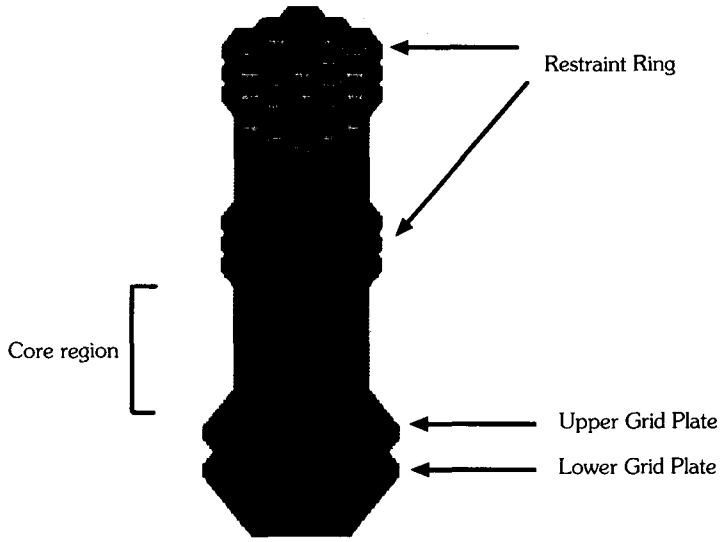

Fig. 2. Core Restrain System Concept (limited-free bow system)

2. Duct Bending

2.1. Duct Model

The duct is modeled as a straight beam, which has thermal and inelastic deflection. When contact occurs due to duct deflection, the load pad represented by a springs transfers the contact force to a neighbor duct(see Fig. 3). Each duct is arrayed with the same stiffness and gap distance. These beam structures are axially subdivided in the user-specified number of finite elements. The finite element analysis is performed under the following assumptions:

1. The duct is considered as a 2 dimensional beam
2. During duct bowing, there is no change of the hexagonal duct shape
3. There is no torsional force in the normal direction.
4. Fuel rod does not affect on the duct stiffness.
5. The friction force at the contact face of the load pad was ignored.

In order to calculate the contact, each assembly duct is subdivided into cells at each node point. The stress and strain, due to creep and swelling calculated in each cell, and the sum of the moments

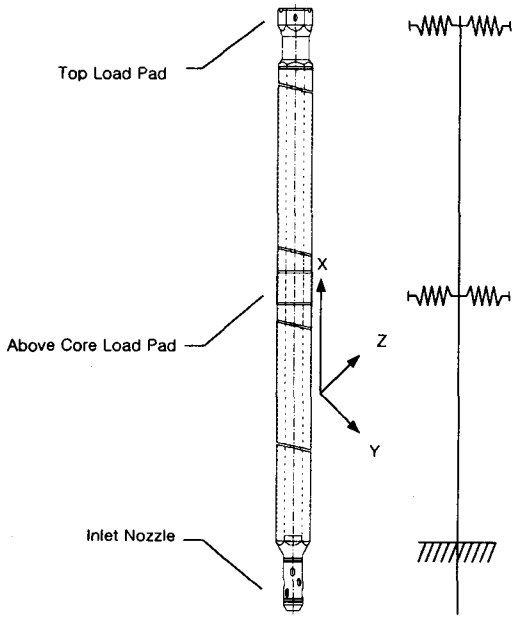

Fig. 3. KALIMER Assembly Duct Model

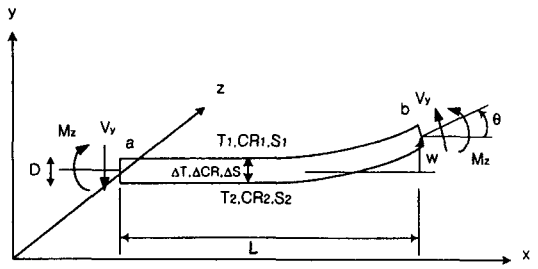

Fig. 4. Beam Element Bow Deflection Model

through all the cross sections of the hexagonal duct, determine the deflection of the beam.

2.2. Bending Model

Self-bending moments by thermal gradients, differential creep and swelling are solved numerically to give an unrestrained bow deflection of each finite beam elements. Constrained bowing and the resulting interaction forces are calculated based on a simple force balance and the deflection compatibility criteria for the assembly ducts. Thermal bowing is developed by thermal moment M_T, due to the temperature difference between the upper face and lower face of the finite beam element(see Fig. 4). M_T is given as[9]:

$$M_T(x) = E(x)\alpha(x)\int_A T(x,y)ydA = \frac{\alpha(x)\Delta T(x)E(x)I(x)}{D(x)} \quad (1)$$

where $E(x)$ is Youngs modulus, $\alpha(x)$ is the thermal expansion coefficient, $T(x,y)$ is the temperature at location x, y, T is the temperature difference between two sides wall, $I(x)$ is the moment of inertia of the finite beam element, and $D(x)$ is the beam element diameter.

The thermal bow of the beam is calculated by using the conventional beam bending theory. From thermal moment M_T, the thermal bow shape of finite beam element is calculated as follows:

$$\frac{d^2V_T}{dX^2} = \frac{M_T(X)}{E(T)I(X)} = \frac{\alpha(T)\Delta T(X)}{D(X)} \quad (2)$$

The creep and swell bow shape of the finite beam element is calculated by creep moment M_{CR} and swelling moment M_S from ΔCR, ΔSW (see Fig. 4).

$$\frac{d^2V_{CR}}{dX^2} = \frac{M_{CR}(X)}{E(T)I(X)} = \frac{\Delta CR(X)}{D(X)} \quad (3)$$

$$\frac{d^2V_S}{dX^2} = \frac{M_{SW}(X)}{E(T)I(X)} = \frac{\Delta SW(X)}{D(X)} \quad (4)$$

Using bow shapes of the finite beam element, bow displacement of each node can be calculated in the NUBOW-2D KMOD. The unrestrained bow displacement of node is calculated from the centerline displacement, w, the length of finite element, distance between and centerline bending angle (see Fig 4). Whole Bow shapes of ducts are calculated using superposition of the displacement of node. Bow displacement of each node of finite beam elements and duct bow shapes are shown as follows:

- Thermal bow deflection

$$w_i = \frac{\alpha(\Delta T_{i-1}/D_{i-1})\ell^2}{3} + \frac{\alpha(\Delta T_i/D_i)\ell^2}{6} \quad (5)$$

$$V_{ih}(i) = \frac{\alpha(\Delta T_{i-1}/D_{i-1})\ell^2}{3} + \frac{\alpha(\Delta T_i/D_i)\ell^2}{6} + \theta\ell + V_{ih}(i-1) \quad (6)$$

- Inelastic bow deflection

$$w_i = \frac{C_{i-1}\ell^2}{3} + \frac{C_i\ell^2}{6} \quad C = \int_I \frac{y}{I}(\varepsilon_c + \varepsilon_s)dA \quad (7)$$

$$V_{inel}(i) = \frac{C_{i-1}\ell^2}{3} + \frac{C_i\ell^2}{6} + \theta\ell + V_{inel}(i-1) \quad (8)$$

The constraint bow shape due to duct interaction can be calculated using the equilibrium condition

$M_{i+1}=M_i+ V_i\ell$, $Mi = M_{i+1} - V_{i+1}\ell$,

- Mechanical bow deflection

$$w_i = \frac{1}{EI}\int_0 M dx^2 = -\frac{Ml^2}{2EI} + \frac{Vl^3}{3EI} \tag{9}$$

$$VB(i) = \left(\frac{M}{2} + \frac{F\ell}{3}\right)\frac{\ell^2}{I} + \theta\ell + VB(i-1) \tag{10}$$

where w is the each finite element node displacement, is the centerline bending angle, and $V_{th}(i)$, $V_{inel}(i)$, and $VB(i)$ are the thermal, inelastic, and mechanical displacements obtained from bow shapes of the duct.

When unrestrained bows are larger than the interduct clearance, interaction between the assembly ducts occurs. These interaction forces are given by:

$$P_{ij} = \left(V_{ij}^{th} + V_{ij}^{inel} - V_{ij-1}^{th} - V_{ij-1}^{inel} - d_{ij}\right)K_{ij} \tag{11}$$

where P_{ij} is the contact force, d_{ij} is the interduct gap, and K_{ij} represents contact spring stiffness which is obtained by using ANSYS program analysis. The contact spring stiffness of ACLP and TLP of KALIMER duct is 1.64×10^5 N/mm, 1.7×10^7 N/mm.

The contact forces at 21 node points, P_{ij}, can be obtained by solving the following matrix equation;

$$\begin{Bmatrix} F_{x_1} \\ M_1 \\ F_{x_2} \\ M_2 \\ F_{x_3} \\ M_3 \\ F_{x_4} \\ M_4 \\ \cdot \\ \cdot \\ F_{x_{21}} \\ M_{21} \end{Bmatrix} = \frac{EI}{\ell^3} \begin{bmatrix} 12 & 6\ell & -12 & 6\ell & & & & & & & & & & & & & & & & & \\ 6\ell & 4\ell^2 & -6\ell & 2\ell^2 & & & & & & & & & & & & & & & & & \\ -12 & -6\ell & 12+12 & -6\ell+6\ell & -12 & 6\ell & & & & & & & & & & & & & & & \\ 6\ell & 2\ell^2 & -6\ell+6\ell & 4\ell^2+4\ell^2 & -6\ell & 2\ell^2 & & & & & & & & & & & & & & & \\ & & -12 & -6\ell & 12+12 & -6\ell+6\ell & & & & & & & & & & & & & & & \\ & & 6\ell & 2\ell^2 & -6\ell+6\ell & 4\ell^2+4\ell^2 & & & & & & & & & & & & & & & \\ & & & & & & \cdot & & & & & & & & & & & & & & \\ & & & & & & & \cdot & & & & & & & & & & & & & \\ & & & & & & & & 12+12 & -6\ell+6\ell & -12 & 6\ell & & & & & & & & \\ & & & & & & & & -6\ell+6\ell & 4\ell^2+4\ell^2 & -6\ell & 2\ell^2 & & & & & & & & \\ & & & & & & & & -12 & -6\ell & 12+12 & -6\ell+6\ell & -12 & 6\ell & & & & & \\ & & & & & & & & 6\ell & 2\ell^2 & -6\ell+6\ell & 4\ell^2+4\ell^2 & -6\ell & 2\ell^2 & & & & & \\ & & & & & & & & & & -12 & -6\ell & 12 & -6\ell & & & & & \\ & & & & & & & & & & 6\ell & 2\ell^2 & -6\ell & 4\ell^2 & & & & & \end{bmatrix} \begin{Bmatrix} dx_1 \\ \theta_1 \\ dx_2 \\ \theta_2 \\ dx_3 \\ \theta_3 \\ dx_4 \\ \theta_4 \\ \cdot \\ \cdot \\ dx_{21} \\ \theta_{21} \end{Bmatrix} \tag{12}$$

2.3. Material Property Model

HT9 steel(martensitic stainless steel) is used as the structural material of the assembly duct for KALIMER. The material properties of HT9 including creep, swelling, Youngs modulus and thermal expansion were installed into NUBOW code. The material properties of HT9 that were used in the code are as follows;

$$E = 2.425\times10^5 - 102.9T \tag{13}$$

$$\alpha(T) = 5.678\times10^{-6} + 1.6222\times10^{-8}T - 7.728\times10^{-12}T^2 \tag{14}$$

$$\dot{\varepsilon}_{cr} = \left[-2.9 + 9.5\times10^{-3}\times(T-273)\right]\times10^{-26}\phi\sigma^{1.3} + 1.743\times10^{18}\left(\sigma/E(T)\right)^{2.3}\exp(-36739/T) \tag{15}$$

where α, E(T), $\dot{\varepsilon}_{cr}$, ϕ, σ, and T are thermal expansion coefficient, elastic modulus(MPa), effective strain rate (%s^{-1}), fast neutron flux ($n\cdot cm^{-2}s^{-1}$), effective stress(MPa), and temperature(°K), respectively[10].

During LMR operation, the amount of neutron irradiation is reported approximately ~100dpa, however, the peak swelling rate under steady state condition is recommended as 0.6% up to 100dpa [11, 12]. This value was used in this program.

3. Results and Discussions

Under LMFBR irradiation environments, duct bowing occurred by thermal expansion, creep, and the swelling of the duct material(HT9). At the initial core, KALIMER fuel assembly ducts normally experience a temperature difference of ~20℃ between the duct walls at the radial blanket assembly duct and shield assembly duct region where the outlet temperature is ~530℃. The bending moment generated by the difference of the thermal expansion, creep, and swelling of the duct between the interfacial walls causes duct

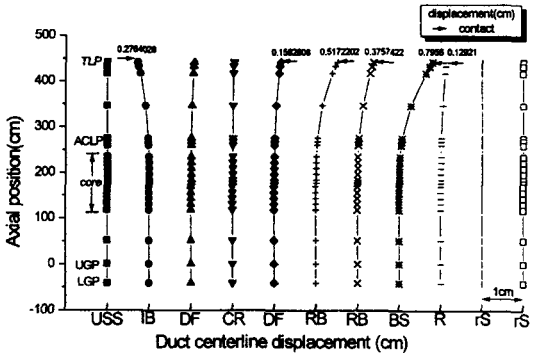

Fig. 5. Thermal Bowing of the Assembly Duct(outlet temperature 530℃)

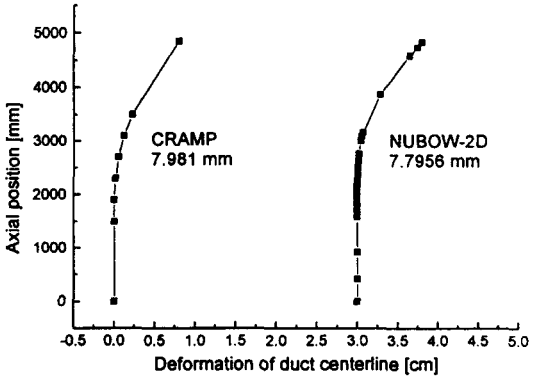

Fig. 6. Thermal Bow Deflection of CRAMP and NUBOW-2D KMOD Code

deflection and if this deflection is lager than between neighbor ducts gap distance, contact between the ducts may occur. Fig. 5 shows the thermal bowing of the duct due only to the difference of the thermal expansion of the duct material at the initial core. The largest duct deflection developed at the 8th shield duct(BS, B4C Shield duct) and its TLP(Top load pad) deflection is about 8mm. Since the initial duct to duct gap distance is 1mm at the load pad, interactions between the ducts occurred and the contact force developed. Fig. 6 and Fig. 7 shows the result calculated by CRAMP code(UK' s core

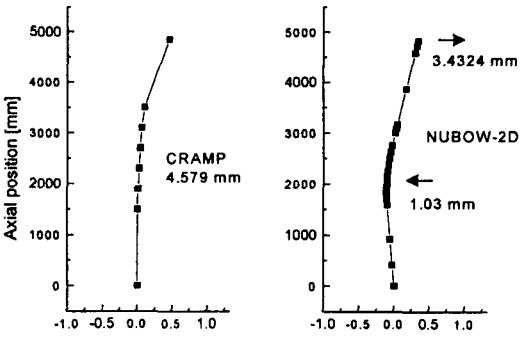

Fig. 7 Duct Bow Deflection After 450 Days

mechanics design tool, 3dimensional code) and NUBOW-2D KMOD. At the 8th shield duct, thermal bow deflection of two codes is showed about 8mm(Fig. 6), and after 450 days, inelastic bow deflection is showed about 4.5 mm(Fig. 7). Although the result of the CRMAP code bigger than that of NUBOW-2D KMOD, considering that CRAMP code is 3 dimensional analysis code, which show well agreement.

The stress developed by the contact force at the duct wall relaxed by creep. When the temperature goes down, these deflections disappear, because the thermal bowings are elastic deformation. Even though the elastic bow deflections disappear, permanent bow deflections due to creep and swelling remain. Fig. 8 shows the bow shapes of the ducts in normal operation conditions and the shut down equilibrium state at 450 days. In Fig. 8, each line mean duct which has no thickness and show the deflection of duct center line. The x axis start point of each line has each gap distance(1mm) between ducts plus outward strain value of the thermal expansion of grid plate. In order to minimize duct bowing, several design parameters concerning geometrical conditions, ACLP(Above Core Lode Pad) position, the gap distance between ducts, and the gap distance between the duct and restraint ring were selected

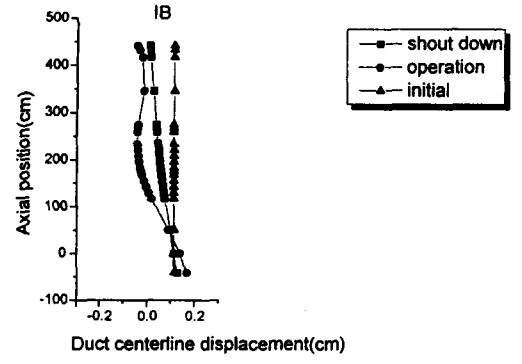

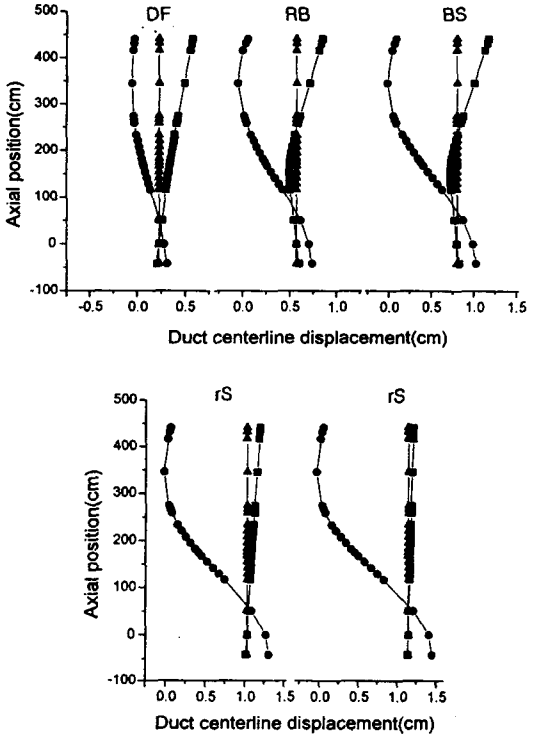

Fig. 8. Bow Shapes at Reactor Shout Down (at 450 days)

and calculated under KALIMER operation conditions.

3.1. Bow tendency by ACLP position

After 450 days, Fig. 9 shows each bow shape

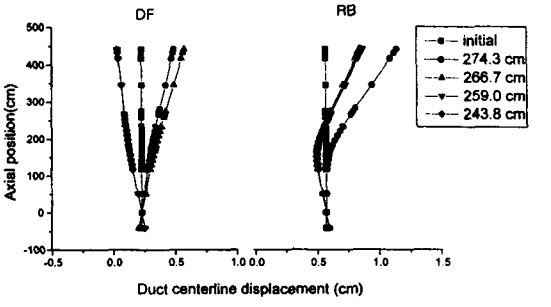

Fig. 9. Bow Shape of the Duct by ACLP Position (at 450 days)

with each axial position of ACLP(245cm, 260cm, 267cm, and 275cm) at reactor shout down. As the axial position of the ACLP is closer to the fuel level, it appears that the bowing of the ducts are small. The 2nd inner blanket(IB) assembly duct shows about 0.4mm displacement difference of duct top and the 6th radial blanket assembly duct shows about 3.5mm displacement difference of duct top. Duct bending developed by bending moment, mainly generated by thermal expansion and irradiation induced swelling at the fuel level of the duct material. Because the moment is proportional to the beam element length, it is reasonable that the ACLP is closely positioned at the fuel level.

3.2. Gap Distance Between the Assembly Ducts

During the refueling operation, the withdrawal force of ducts may become twice or three times as large as their own weight due to assembly ducts cluster tightness. To evaluate the duct bow shape, the duct gap distance is changed to 1mm, 1.5mm, 2mm, and 2.5mm. Fig. 10 shows each bow shape of the gap distance at 450 days. A wide gap distance between the assembly ducts is favorable for reducing the bowing loads. However, if the gap distance is more than 2mm, the 5th driver

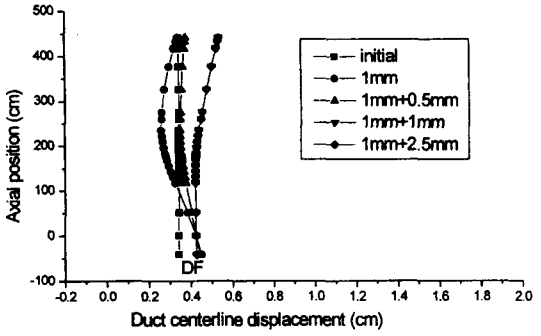

Fig.10. Bow Shape of the Duct by Interduct Gap Distance(at 450 days)

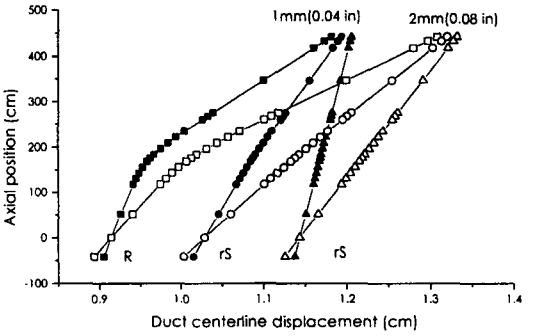

Fig. 11. Bow Shape of the Duct by Gap Distance Between the Duct and Restraint Ring

fuel duct has a large enough gap to deform freely.

3.3. Gap distances Between the Assembly Duct and Restraint Ring

The gap distances between the assembly duct and restraint ring are changed to 1mm, and 2mm. Fig. 11 shows the bow shapes of the duct according to each gap distance. Since the temperature and neutron flux is not comparatively high outside of the core, permanent bending of the ducts is small. The contact force also largely decrease at ACLP and TLP. As shown in Fig. 11, if the gap distance between the duct and restraint ring increases, permanent bending curvature decreases about 10%.

4. Summary and Conclusions

The material properties of HT9, which is a structural material for the assembly duct of KALIMER, are modeled and the model is installed into the NUBOW2D KMOD. The mechanical behavior of assembly ducts related to several design parameters are evaluated. ACLP positions, the gap distance between the ducts, and the gap distance between the duct and restraint ring were selected as the sensitivity parameter for the evaluation of duct deflection.

At the initial core, bending moment that is generated by the thermal expansion of the assembly duct wall develops duct bowing. When this bowing exceeds the gap distance between neighboring ducts, the assembly ducts interact with each other. As time increases, the permanent residual bow is increased primarily due to irradiation enhanced creep during core operation. As the axial position of the ACLP is closer to the top level of the fuel, the bowing of the ducts are small. Though the displacement of the TLP increase, the wider gap distance between duct and restraint ring is favorable for reducing the duct bowing.

Acknowledgment

This work has been carried out under the national nuclear long-term R&D program which is supported by the Korea MOST(Ministry of Science and Technology).

Reference

1. S. A. Kamal and Y. Orechwa, Transient Bowing of Core Assemblies in Advanced liquid Metal Fast Reactors, Proc. Topl. Mtg. Reactor

Physics and safety, Saratoga Springs, New York, USA, September 17-19, 1986, NUREG/CP-0080, Conf-860906-21, (1986).
2. J. H. Bottcher, G. L. Hofman, Subassembly Bowing Experience in EBR-II.
3. R. C. Perrin, J. C. Duthie, The core restraint modelling program CRAMP part 1 : general description and user manual, MRL-R-2030(s)part 1, UKAEA, August (1989).
4. R. Menssen, DDT-A 3-Dimensional Program for The Analysis of Bowed Reactor Cores, Fourth Intl. Conf. on Structural Mechanics in Reactor Technology, San Francisco, USA, August 15-19, D 2/4. (1977).
5. M. Nakagawa, ARKAS: A Three-Dimensional Finite Element Program for Core-Wide Mechanical Analysis of Liquid-Metal Fast Breeder Reactor Cores, Nucl. Tech. 75,46(1986).
6. McLENNAN, G. A., NUBOW-2D Inelastic: A Computer Program for the Bowing History of reactor Cores, Trans. Am. Nucl. Soc., Vol.27 P.756(1977).
7. S. A. Kamal and Y. Orechwa, Transient Bowing of Core Assemblies in Advanced Liquid Metal fast Reactors. Conf-860906-21,(1986).
8. B. O. Lee et al., The comprehensive Analysis on the Thermo-mechanical Behavior of the Assembly Ducts by 2D and 3D code , Proceedings of the Korean Nuclear Society Spring Meeting, Kori, Korea, May26-27(2000).
9. B. A. Boley and J. H. Weiner, Theory of Thermal Stresses, John Wiley & Sons, Inc., (1960).
10. Hwang, W., Lee, B.O., Nam, C., and Paek, S.K., KALIMER Fuel System Perliminary Design Description, KALIMER/FD700-DD-01/1998 (FD19000000) Rev.0, Aug. (1998).
11. D. S. Gelles, Swelling in Several Commercial Alloys Irradiated to Very High Neutron Fluence, HNM 122&123, 207-213(1984).
12. D. S. Gelles, and R. L. Meinecke, Swelling in Simple Ferritic Alloys Irradiated To High fluence, DOE/ER-0045.